A Generic Dynamic Load Model Framework

You Lin and Jianhui Wang

***Abstract*—Formulating accurate dynamic load models is critical for power system analysis, control, and planning. In this paper, a generic dynamic load model is proposed. The dynamic power response of the load is directly approximated as the superposition of various mathematical functions that produce a dynamic response. Basic physical principles of the dynamic process are reflected in the mathematical functions utilized in the proposed model. First, different stages of the dynamic process are detected based on the continuity of derivatives of the measurement. Second, a complete set of mathematical functions that produce the dynamic responses in electric devices are formulated. Third, a parsimonious set of mathematical functions is selected at each stage by performing feature selection using nonlinear principal component analysis. The proposed model is further formulated based on the parsimonious set of mathematical functions at each stage. Finally, the parameters of the proposed model corresponding to different system events are solved. Based on the formulated model, its possible application in event detection is further analyzed. The proposed model is easy to implement given limited data measurement. Various tests on different system event data are performed to validate the effectiveness of the proposed model. The results show that the proposed model has excellent accuracy and robustness for different system events.**

***Index Terms*—Approximation, dynamic process, generic framework, load model, physical principle.**

I. Introduction

LOAD modeling for power system is to reproduce the power response given system variations. Load modeling is not a forecasting problem but an optimization problem that searches for optimal and robust models to produce dynamic load behavior corresponding to unforeseen system events [1]. Accurate load modeling for power system is critical for power system analysis and control.

From the perspective of constructing a load model structure, relevant methods can be divided into two categories: component-based and measurement-based [1]. The component-based methods are formulated based on the physical behaviors of individual load components such as the induction motors. In [2], a robust method is proposed to identify the time-varying parameters of the synthesis load modeling based on a nonlinear least-square algorithm. An open-source Western Electricity Coordinating Council (WECC) composite load model is implemented in GridPACK™ in [3], in which high-performance computing and parallel simulation are applied. In [4], a two-stage method based on deep reinforcement learning is proposed to solve optimal parameters of the WECC load model. In [5], a tensor-based parameter estimation method is proposed to estimate globally optimal parameters and perform a sensitivity analysis of the constant impedance, constant current, and constant power (ZIP) + induction motor (IM) load model. The advantage of the component-based method is that it requires a small amount of measurements to find optimal models with good robustness. However, because of the increasing integration of distributed energy resources and power electronic devices on the load side, more load components are expected to supplement the component-based load models [6], [7], which will add dozens of more parameters. Due to the high nonlinearity and high dimensionality, it is difficult to obtain accurate component-based models. In comparison, the measurement-based methods formulate the relationship between input and output depending on data-driven techniques such as statistical methods, machine learning algorithms, and the powerful deep learning algorithms [8]-[10]. In [11], a neural network-based method is proposed to model the highly nonlinear characteristics of the bulk load such as electric arc furnaces. The advantage of these methods is that no physical details of the electrical device are required. However, the data-driven techniques may need a massive number of measurements, which is difficult to obtain in the real system [12]. Without a comprehensive data set, the measurement-based models may have low robustness for unforeseen events.

In this paper, a generic dynamic load model is proposed based on the superposition of mathematical functions representing basic physical principles of the dynamic process. The proposed model is easy to implement, requires less computation resource and system measurements, and has excellent accuracy and robustness. The proposed model assumes that the voltage, active power, and reactive power can be measured in the system buses. Since the dynamic load model is to reproduce the load behavior in all event scenarios, the measurements should include at least limited categories of faults. The proposed model is easy to reproduce and can provide a good benchmark model for academic research and real applications. The contributions of this paper are as follows.

1) Basic physical principles are utilized to formulate the generic dynamic load model based on the superposition of mathematical functions, which makes the proposed model

Manuscript received: August 28, 2020; revised: November 24, 2020; accepted: February 19, 2021. Date of CrossCheck: February 19, 2021. Date of online publication: April 21, 2021.

Y. Lin (corresponding author) and J. Wang are with the Department of Electrical and Computer Engineering, Southern Methodist University, Dallas, USA (e-mail: youl@smu.edu; jianhui@smu.edu).

DOI: 10.35833/MPCE.2020.000642

very robust and accurate.

2) The proposed model is easy to implement without strong computation requirement or system modeling effort.

3) The unique characteristics and similarities among different system events are delineated, providing a valuable reference for detecting various system events.

The remainder of this paper is organized as follows. Section II describes the detailed structure of the generic dynamic load model, selection of mathematical functions, and parameter estimation. Section III performs various tests on different system events to validate the effectiveness of the proposed model, and it also provides a comprehensive discussion of the potential of the proposed model for event detection. Finally, Section IV concludes this paper.

II. Generic Dynamic Load Model

The load response can be approximated as a superposition of various mathematical functions producing dynamic responses to an external input such as voltage or frequency since the underlying physical equations for almost every component are known in a load composition. To avoid solving complicated differential equations, the relationship between the active power response $P(t)$ at time t and the system measurement vector $\boldsymbol{M}$ such as bus voltage, is approximated based on the superposition of mathematical functions, as shown in (1). The mathematical function $\phi_k(\theta_k, M_t, t)$ is formulated considering the physical principles of various electrical components. This section will introduce how to choose the parsimonious set of mathematical functions and formulate the generic dynamic load model.

$$P(t) \approx \boldsymbol{\omega}^{\mathrm{T}} \boldsymbol{\phi}(\boldsymbol{\theta}, \boldsymbol{M}, t) = \sum_{k=1}^{K} \omega_k \phi_k(\theta_k, M_t, t) \tag{1}$$

where K is the number of mathematical functions; $\boldsymbol{\omega} = [\omega_1, \omega_1, \ldots, \omega_K]^{\mathrm{T}}$, which is the vector of weights ω_k of the generic dynamic load model; $\boldsymbol{\theta} = [\theta_1, \theta_2, \ldots, \theta_K]^{\mathrm{T}}$, which is the vector of parameters θ_k of the generic dynamic load model; M_t is the element of $\boldsymbol{M}$; and $\boldsymbol{\phi}(\cdot) = [\phi_1(\cdot), \phi_2(\cdot), \ldots, \phi_K(\cdot)]^{\mathrm{T}}$, which is the vector of mathematical functions $\phi_k(\cdot)$.

A. Candidate Mathematical Functions

The dynamic response of load corresponding to system operations falls in three categories: slow and smooth change, abrupt change, and damping.

1) Slow and Smooth Change

The slow and smooth change in a system causes gradual variations. Any slow and smooth change can be fitted by superimposing multiple functions. Polynomial and trigonometric functions can be practical, which are widely used in load components.

2) Abrupt Change

Compared with slow and smooth changes, abrupt changes are the sudden ones that occur instantly. When a dynamic system suddenly transfers from a steady state to a new state, an abrupt change occurs. Once an abrupt change occurs, it will trigger very different system behaviors and produce system discontinuity. Therefore, the abrupt changes can be detected by searching the discontinuous data points of system measurements. In system components, the sudden internal or external force can induce an abrupt change of voltage and current in a power system, e. g., the short or open circuit caused by overloading, external natural factors, and automatic or manual control measures. This abrupt change can be the original force and the beginning of a new dynamic process. It means that the sudden force not only occurs when a system contingency occurs but also appears when system controls are triggered in the process of recovering to the stable operation or collapsing. Therefore, it is essential to identify such a sharp change and divide the dynamic process into different stages to accurately describe the system behaviors at different stages with different initial conditions.

As the derivatives of data series provide rich information on the abrupt changes in the data, all derivatives are studied, including the independent derivatives of voltage and active power, the dependent relationships of voltage derivatives and voltage, and the dependent relationships of voltage derivatives and active power. Each dependent relationship reflects a specific physical meaning. One example of the curve reflecting the scaled voltage and its derivative in one-phase fault is presented in Fig. 1(a). In this example and all simulations in the following sections, all data are normalized based on the rated values.

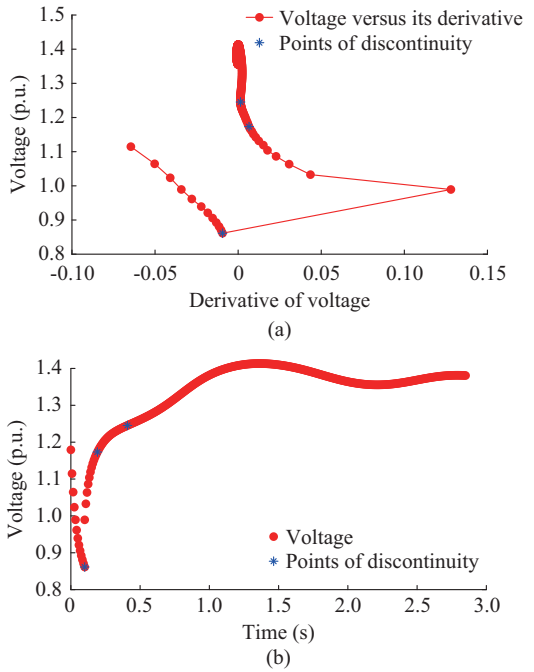

Fig. 1. Normalized voltage versus its derivative and dynamic voltage curves. (a) Voltage versus its derivative. (b) Dynamic voltage curve.

As shown in Fig. 1, discontinuities can be detected in this system, and these discontinuities are marked as blue points. There are three data points of discontinuity in this system. Each data point reflects one abrupt change in the system. These abrupt changes divide the voltage curve into four stages, as shown in Fig. 1(b). It is easy to observe that the first point leads to a more significant and more apparent abrupt change than the others. The corresponding time of the first

point is precisely the fault clearing time, demonstrating the physical meaning of the discontinuous data points.

3) Damping

After abrupt changes occur, the system tends to oscillate. Damping has the effect of preventing, limiting, and reducing the oscillations of the vibratory system [13]. Exponential functions e^{xt}, reciprocal $1/x$, Gaussian function, etc., are potent functions for describing system damping in engineering. x is the voltage or its derivative. The dynamic process of power system load is quite similar to the trajectory of the damped sinusoidal oscillation curve.

Except for the above candidate mathematical functions producing dynamic process, other commonly used mathematical functions are also a useful reference for curve fitting, e.g., cardioid and equiangular spiral curves [14].

From the above analysis, the following functions are selected as the complete set of candidate mathematical functions: ① the polynomial function $a_0+a_1x+\ldots+a_nx^n$; ② the trigonometric function $b_1\cos(b_2(x+b_3))$; ③ the exponential function $c_1e^{c_2x+c_3}$; ④ the product of any combination of the above three kinds of functions, e. g., $(a_0 + a_1x + \ldots + a_nx^n)\cos(b_2(x + b_3))$; ⑤ other mathematical curve functions. a_i, b_i, and c_i are the parameters of candidate mathematical functions.

B. Selecting Parsimonious Set of Mathematical Functions

After determining the candidate mathematical functions, it is essential to select a parsimonious set of mathematical functions. Since it is very challenging to find optimal parameters of the superposition of all functions, a feature selection algorithm is utilized to select the parsimonious set of mathematical functions. The nonlinear principal component analysis (NLPCA) is a robust feature selection algorithm for reducing data dimensionality, which has excellent performance on dealing with nonlinear data sets [15]. Therefore, NLPCA is utilized to determine the principal functions.

The proposed model is then formulated by superposing the selected parsimonious set of mathematical functions, as shown in (1). The corresponding parameters of the proposed model can be easily calculated using nonlinear curve fitting algorithms. In this paper, the nonlinear least-squares solver in MATLAB [16] is applied to solve optimal parameters in the proposed model.

C. Structure of Proposed Model

The structure of the proposed model is as follows.

1) Identify abrupt changes by analyzing the data derivatives such as the derivative of bus voltage.

2) Divide the data set into different stages according to the identified abrupt changes of the data.

3) Determine the complete set of the candidate mathematical functions as mentioned in Section II-A-3). Select a parsimonious set of mathematical functions from the complete set of the candidate mathematical functions utilizing the NLPCA.

4) Formulate the proposed model by superposing the parsimonious set of mathematical functions, as shown in (1).

5) Calculate optimal parameters of the proposed model utilizing the nonlinear least-squares algorithm.

III. Case Studies

Various tests are performed with different categories of faults at different locations. The simulated system is the IEEE 39-bus system with a WECC composite load model connected at Bus 20. Various contingencies at different buses are simulated, including a single-phase ground fault, a two-phase-to-ground fault, and a three-phase fault performed separately on Buses 6, 14, and 21, respectively. The transient security assessment tool (TSAT) in DSATools [17] is utilized to perform all the contingency simulations. In the simulation of the proposed model and the benchmark models, the data of the single-phase ground fault of Bus 6 is used to train the model. The trained model is applied to other cases such as the case where a single-phase ground fault is performed on Bus 14 and Bus 21, to compare the performance of the proposed model and the benchmark models.

A. Abrupt Change Identification

Abrupt changes are identified based on the voltage derivatives, which are presented in Fig. 1. Abrupt changes are identified at 0.1 s, 0.1917 s, and 0.4083 s, respectively, as indicated by blue points in Fig. 1(a). These abrupt changes divide the dynamic process into four stages, as shown in Fig. 1(b).

B. Generic Functions of Dynamic Load Model

In this paper, the complete set of the candidate mathematical functions is set as:

$$\begin{aligned}\{&a_0+a_1x+\ldots+a_nx^n, b_1\cos(b_2(x+b_3)),\\ &c_1e^{c_2x}, (a_0+a_1x+\ldots+a_nx^n)c_1e^{c_2x},\\ &(a_0+a_1x+\ldots+a_nx^n)c_1e^{c_2x}b_1\cos(b_2(x+b_3)),\\ &j_1(j_2x+j_3)^{2/3}, \sqrt{l_1^2+(l_2x+l_3)^2}\}\end{aligned} \tag{2}$$

where j_i and l_i are the parameters of candidate mathematical functions. It should be noted that any order polynomial functions can be selected. Only the first-order voltage derivative is considered since the first-order derivative can produce enough high accuracy in the proposed model.

Using the NLPCA, the parsimonious set of mathematical functions is determined. Among all the functions in the complete set shown above, the functions indicating principal features are selected to construct the parsimonious set of mathematical functions at each stage of the proposed model. Therefore, different parsimonious sets of mathematical functions will be chosen at different stages. In the proposed model, the linear polynomial function has good performance. Thus, only the linear polynomial function is selected to represent the polynomial functions. The parsimonious set at stage 1 is $\{a_0+a_1x, b_1\cos(b_2(x+b_3))\}$. The parsimonious set at stage 2 is the same as stage 1. At stage 3, the parsimonious set is $\{a_0+a_1x, j_1(j_2x+j_3)^{2/3}, \sqrt{l_1^2+(l_2x+l_3)^2}\}$, while it is $\{a_0+a_1x\}$ at stage 4. The proposed model is formed by superposing the mathematical functions in the selected parsimonious sets, as shown in (3). By combining the coefficients, the proposed

model in (3) can be further simplified as (4). Optimal parameters of the proposed model are solved using the nonlinear least-squares algorithm.

$$S_{PQ}=\begin{cases} w_{11}(a_0+a_1x)+w_{12}b_1\cos(b_2(x+b_3)) & \text{stage 1}\\ w_{21}(a_0+a_1x)+w_{22}b_1\cos(b_2(x+b_3)) & \text{stage 2}\\ w_{31}(a_0+a_1x)+w_{32}j_1(j_2x+j_3)^{2/3}+ & \\ \quad w_{33}\sqrt{l_1^2+(l_2x+l_3)^2} & \text{stage 3}\\ a_0+a_1x & \text{stage 4}\end{cases} \tag{3}$$

$$S_{PQ}=\begin{cases} a_{11}+a_{12}x_1+a_{13}\cos(a_{14}(x_1+a_{15})) & \text{stage 1}\\ a_{21}+a_{22}x_1+a_{23}\cos(a_{24}(x_1+a_{25})) & \text{stage 2}\\ a_{31}+a_{32}x_2+a_{33}(a_{34}x_2+a_{35})^{2/3}+ & \\ \quad a_{36}\sqrt{a_{37}^2+(a_{38}x_2+a_{39})^2} & \text{stage 3}\\ a_{41}+a_{42}x_2 & \text{stage 4}\end{cases} \tag{4}$$

where S_{PQ} is the active power P or reactive power Q; ω_{ij} is the weight of the j^{th} candidate mathematical function at stage i; x_1 is the bus voltage; x_2 is the bus voltage derivative; and a_{ij} is the parameter of the proposed model.

C. Robustness of Proposed Model

The estimated active and reactive power curves calculated from the proposed model (4) are presented in Figs. 2-5, which correspond to different fault types with the fault location at Bus 6 or Bus 21. The normalized root mean square errors (NRMSEs) of the estimated active and reactive power in different fault scenarios are presented in Tables I and II, respectively. The dynamic power curves for different fault types with fault location at Bus 21 are quite different from those at Bus 6. In Fig. 5, the reactive power curve in the single-phase fault is completely different from those in two-phase-to-ground and three-phase faults. The results show that the proposed model has high estimation accuracy, excellent robustness, and good generalization performance at all stages in different fault scenarios.

The traditional ZIP model and the artificial neural network (ANN) model are used as benchmark models and compared with the proposed model. The stage detection strategy is also utilized in the ZIP and ANN models. The same data set is utilized in ZIP, ANN, and the proposed models. The NRMSEs of the three models are presented in Tables I and II. The results show that the proposed model has much lower NRMSEs than the ZIP model in all fault scenarios. The measured data with fault location at Bus 6 are used to train the ANN model. The ANN model only has good accuracy in the fault scenarios that are utilized for training the model. The ANN model in other fault scenarios shows that it has poor robustness.

Furthermore, the polynomial model is selected as the benchmark model to compare with the proposed model. The polynomial regression model is popular in fitting steady-state data based on the polynomial function shown in (5).

$$P=\beta_0+\beta_1x+\ldots+\beta_nx^n \tag{5}$$

where $\beta_0,\beta_1,\ldots,\beta_n$ are the coefficients of the polynomial model.

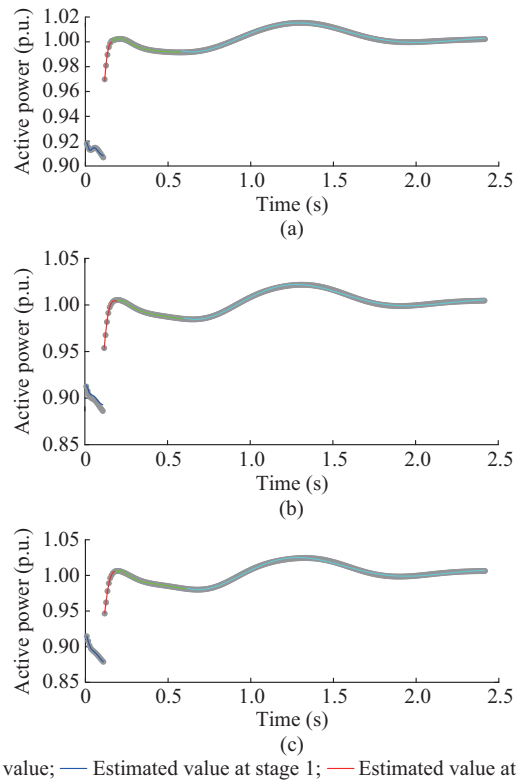

Fig. 2. Estimated active power calculated from proposed model for different fault types with fault location at Bus 6. (a) Single-phase fault. (b) Two-phase-to-ground fault. (c) Three-phase fault.

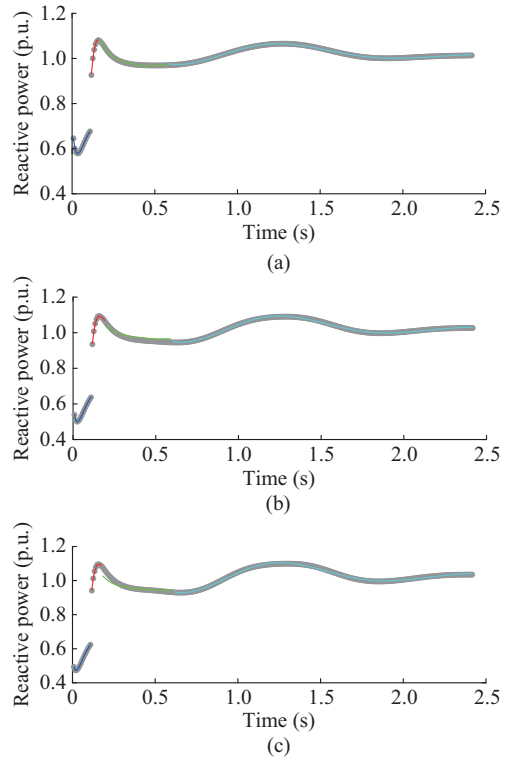

Fig. 3. Estimated reactive power calculated from proposed model for different fault types with fault location at Bus 6. (a) Single-phase fault. (b) Two-phase-to-ground fault. (c) Three-phase fault.

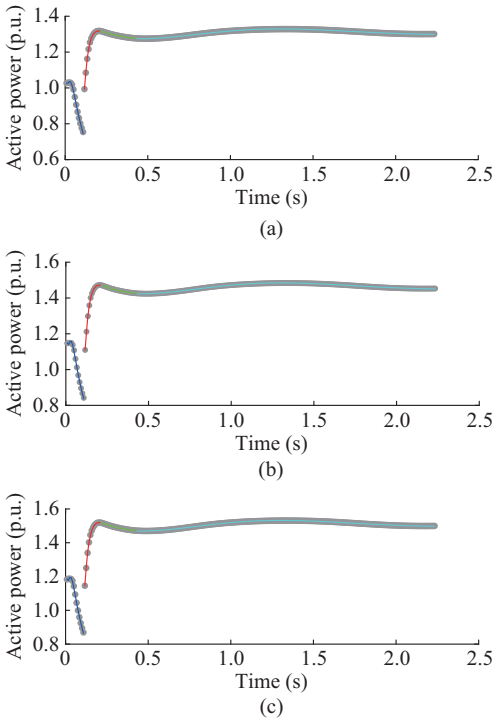

Fig. 4. Estimated active power calculated from proposed model for different fault types with fault location at Bus 21. (a) Single-phase fault. (b) Two-phase-to-ground fault. (c) Three-phase fault.

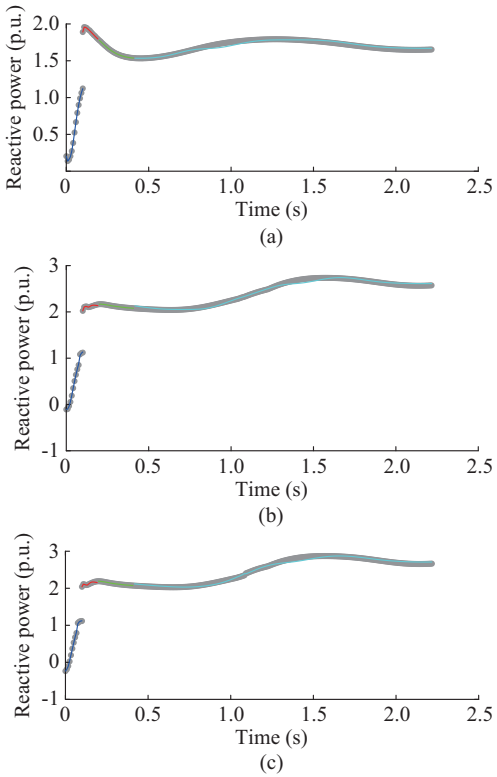

Fig. 5. Estimated reactive power calculated from proposed model for different fault types with fault location at Bus 21. (a) Single-phase fault. (b) Two-phase-to-ground fault. (c) Three-phase fault.

TABLE I
COMPARISON OF NRMSES FOR ESTIMATED ACTIVE POWER OF DIFFERENT MODELS

Fault scenario	NRMSE (%)		
	Proposed model	ZIP model	ANN model
Single-phase fault (Bus 6)	0.045	0.190	0.032
Two-phase-to-ground fault (Bus 6)	0.100	0.270	0.051
Three-phase fault (Bus 6)	0.079	0.260	0.055
Single-phase fault (Bus 14)	0.082	0.250	0.210
Two-phase-to-ground fault (Bus 14)	0.130	0.260	0.180
Three-phase fault (Bus 14)	0.110	0.230	0.220
Single-phase fault (Bus 21)	0.073	0.240	0.190
Two-phase-to-ground fault (Bus 21)	0.110	0.270	0.240
Three-phase fault (Bus 21)	0.092	0.260	0.250

TABLE II
COMPARISON OF NRMSES FOR ESTIMATED REACTIVE POWER OF DIFFERENT MODELS

Fault scenario	NRMSE (%)		
	Proposed model	ZIP model	ANN model
Single-phase fault (Bus 6)	0.084	0.220	0.052
Two-phase-to-ground fault (Bus 6)	0.082	0.320	0.066
Three-phase fault (Bus 6)	0.068	0.340	0.048
Single-phase fault (Bus 14)	0.093	0.280	0.390
Two-phase-to-ground fault (Bus 14)	0.110	0.300	0.400
Three-phase fault (Bus 14)	0.095	0.290	0.350
Single-phase fault (Bus 21)	0.085	0.270	0.420
Two-phase-to-ground fault (Bus 21)	0.120	0.330	0.440
Three-phase fault (Bus 21)	0.120	0.390	0.410

Polynomial models with and without the stage detection strategy proposed in this paper are utilized to compare their performance with the proposed model. The polynomial models have the best estimation accuracy with quartic polynomial functions in this paper. Therefore, quartic polynomial models are utilized as benchmark models and $n=4$ in (5). The estimated active power curves calculated by the polynomial model with and without stage detection strategy in the same fault types are presented in Figs. 6-9. The average NRMSEs of the active and reactive power estimated by the polynomial model are shown in Table III. The results show that the stage detection strategy can greatly improve the estimation accuracy of active power. However, the results show that the polynomial model has much worse robustness than the proposed model in different fault scenarios.

D. Applications in Fault Detection

Different categories of faults at various locations may cause significant differences in the dynamic response of load. However, the same type of fault may produce very similar dynamic responses at different locations. It can be observed that the voltage variations of the two-phase-to-ground fault are closer to the three-phase fault than the single-phase fault, which can be identified qualitatively in Fig. 10.

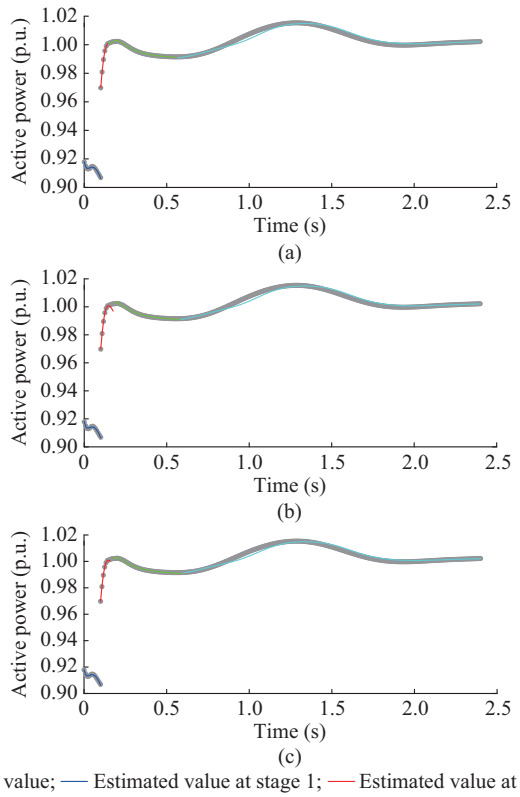

Fig. 6. Estimated active power calculated from polynomial model with stage detection strategy for different fault types with fault location at Bus 6. (a) Single-phase fault. (b) Two-phase-to-ground fault. (c) Three-phase fault.

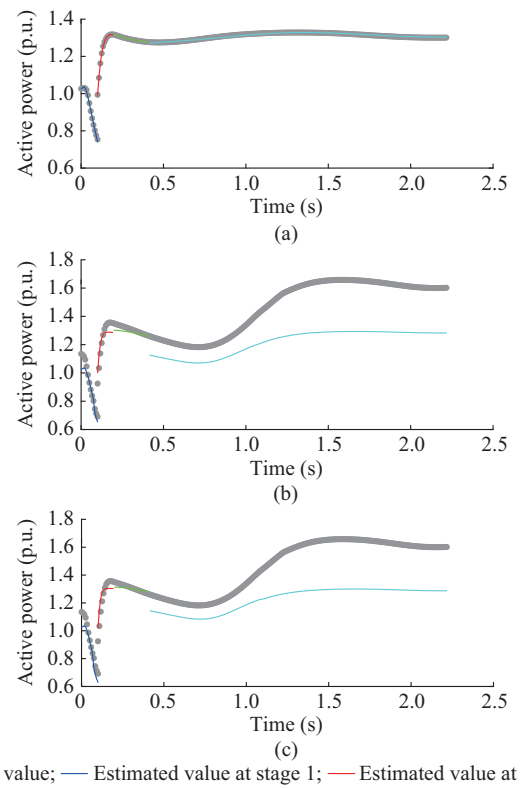

Fig. 7. Estimated active power calculated from polynomial model with stage detection strategy for different fault types with fault location at Bus 21. (a) Single-phase fault. (b) Two-phase-to-ground fault. (c) Three-phase fault.

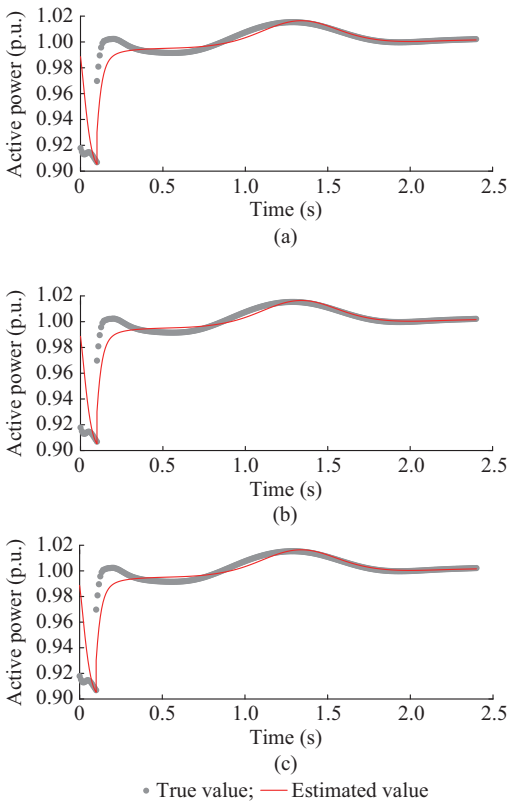

Fig. 8. Estimated active power calculated from polynomial model without stage detection strategy for different fault types with fault location at Bus 6. (a) Single-phase fault. (b) Two-phase-to-ground fault. (c) Three-phase fault.

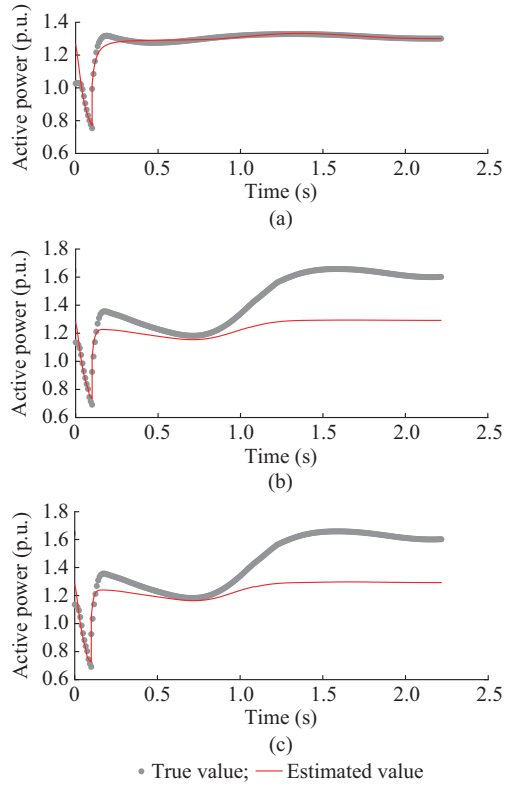

Fig. 9. Estimated active power calculated from polynomial model without stage detection strategy for different fault types with fault location at Bus 21. (a) Single-phase fault. (b) Two-phase-to-ground fault. (c) Three-phase fault.

TABLE III
AVERAGE NRMSES OF ACTIVE AND REACTIVE POWER ESTIMATED BY POLYNOMIAL MODEL WITH AND WITHOUT STAGE DETECTION STRATEGY

Fault scenario	Average NRMSE (%)	
	With	Without
Single-phase fault (Bus 6)	0.17	1.18
Two-phase-to-ground fault (Bus 6)	0.36	1.37
Three-phase fault (Bus 6)	0.32	1.69
Single-phase fault (Bus 14)	0.21	1.25
Two-phase-to-ground fault (Bus 14)	0.29	1.24
Three-phase fault (Bus 14)	0.33	2.21
Single-phase fault (Bus 21)	1.70	1.86
Two-phase-to-ground fault (Bus 21)	23.02	33.83
Three-phase fault (Bus 21)	23.53	33.53

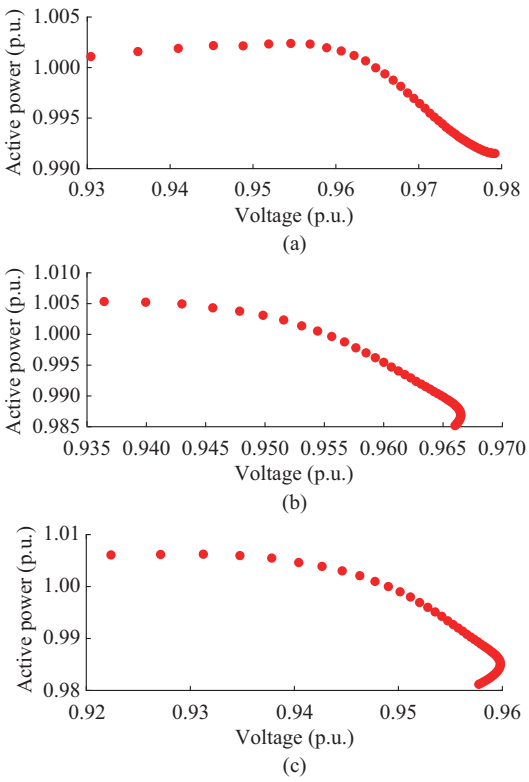

Fig. 10. Dynamic responses of different fault types with fault location at Bus 6 at stage 3. (a) Single-phase fault. (b) Two-phase-to-ground fault. (c) Three-phase fault.

Figure 10 shows that the two-phase-to-ground and three-phase faults have similar dynamic responses, while the single-phase fault has quite different dynamic response. Using the proposed model, it is possible to quantitatively show the similarities and differences of various fault types at different locations, which can be utilized to detect different fault scenarios.

Table IV shows the estimated parameter values of the proposed model in different fault scenarios at stage 2. It should be noted that the value of parameter a_{22} is zero in different fault scenarios. Thus, the parameter a_{22} is not presented in Table IV. Only parameters a_{21}, a_{23}, a_{24}, and a_{25} are shown in Table IV for comparison. The values of parameters a_{23}, a_{24}, and a_{25} in two-phase-to-ground and three-phase fault scenarios are very close, which can be set as the same value in these fault scenarios. Therefore, in future events, if the fair values of parameters a_{23}, a_{24}, and a_{25} are similar, the events have a high probability of two-phase-to-ground and three-phase faults. In contrast, the values of parameters a_{21} and a_{25} have the same values in the single-phase fault scenario, which can be utilized to detect the single-phase fault. The parameter values of the proposed model at other dynamic stages have similar properties.

TABLE IV
ESTIMATED PARAMETER VALUES OF PROPOSED MODEL IN DIFFERENT FAULT SCENARIOS AT STAGE 2

Fault scenario	Parameter value			
	a_{21}	a_{23}	a_{24}	a_{25}
Single-phase fault (Bus 6)	0.970000	0.029600	27.89170	0.925000
Two-phase-to-ground fault (Bus 6)	0.970000	0.034600	25.41180	0.925000
Three-phase fault (Bus 6)	0.970000	0.036400	25.03420	0.925000
Single-phase fault (Bus 14)	1.073997	−0.044140	−16.60360	−0.917442
Two-phase-to-ground fault (Bus 14)	1.108082	−0.045550	−16.07070	−0.947801
Three-phase fault (Bus 14)	1.121513	−0.046080	−15.91240	−0.957614
Single-phase fault (Bus 21)	1.128098	0.189656	13.10717	−1.169593
Two-phase-to-ground fault (Bus 21)	1.259991	0.211831	12.41628	−1.234661
Three-phase fault (Bus 21)	1.300374	0.218619	12.23548	−1.252918

IV. CONCLUSION

In this paper, a generic dynamic load model is derived from the basic physical principles. The proposed model is easy to implement in a real system. The proposed model can be quickly implemented without strong modeling background in an application only with a few data points and minor computation resources. Since it is derived from basic physical principles, it has excellent robustness and generalization capability. The proposed model is demonstrated to have the possibility of detecting different system fault types at different locations. This paper provides a framework on how the generic dynamic load model is formulated. Further work will focus on its robustness verification for more systems and smart detection of different faults. In this paper, the discontinuous data points are selected manually, and the parameters of the model are initialized by experience, which will be further improved to be smarter in discontinuity detection and parameter optimization.

REFERENCES

[1] A. Arif, Z. Wang, J. Wang *et al.*, "Load modeling: review," *IEEE Transactions on Smart Grid*, vol. 9, no. 6, pp. 5986-5999, Nov. 2018.
[2] M. Cui, J. Wang, Y. Wang *et al.*, "Robust time-varying synthesis load modeling in distribution networks considering voltage disturbances," *IEEE Transactions on Power Systems*, vol. 34, no. 6, pp. 4438-4450, Nov. 2019.
[3] Q. Huang, R. Huang, B. J. Palmer *et al.*, "A generic modeling and development approach for WECC composite load model," *Electric Power Systems Research*, vol. 172, pp. 1-10, Jul. 2019.
[4] X. Wang, Y. Wang, D. Shi *et al.*, "Two-stage WECC composite load

modeling: a double deep q-learning networks approach," *IEEE Transactions on Smart Grid*, vol. 11, no. 5, pp. 4331-4344, Sept. 2020.
[5] Y. Lin, Y. Wang, J. Wang *et al*., "Global sensitivity analysis in load modeling via low-rank tensor," *IEEE Transactions on Smart Grid*, vol. 11, no. 3, pp. 2737-2740, May 2020.
[6] North American Electric Reliability Corporation (NERC). (2016, Dec.). NERC draft technical reference document: dynamic load modeling. [Online]. Available: https://www. nerc. com/comm/PC/LoadModelingTaskForceDL/Dynamic% 20Load% 20Modeling% 20Tech% 20Ref% 202016-11-14%20-%20FINAL.PDF
[7] North American Electric Reliability Corporation (NERC). (2017, Sept.). NERC draft reliability guideline: distributed energy resource modeling. [Online]. Available: https://www. nerc. com/comm/PC/LoadModelingTaskForceDL/Reliability_Guideline_-_DER_Modeling_Parameters_-_2017-04-04_-_FINAL_DRAFT.pdf
[8] T. Hiyama, M. Tokieda, W. Hubbi *et al*., "Artificial neural network based dynamic load modeling," *IEEE Transactions on Power Systems*, vol. 12, no. 4, pp. 1576-1583, Nov. 1997.
[9] D. Chen and R. R. Mohler, "Neural-network-based load modeling and its use in voltage stability analysis," *IEEE Transactions on Control Systems Technology*, vol. 11, no. 4, pp. 460-470, Jul. 2003.
[10] Y. Lin and J. Wang, "Probabilistic deep autoencoder for power system measurement outlier detection and reconstruction," *IEEE Transactions on Smart Grid*, vol. 11, no. 2, pp. 1796-1798, Mar. 2020.
[11] G. Chang, C.-I. Chen, and Y.-J. Liu, "A neural-network-based method of modeling electric arc furnace load for power engineering study," *IEEE Transactions on Power Systems*, vol. 25, no. 1, pp. 138-146, Feb. 2010.
[12] M. Khodayar and J. Wang, "Probabilistic time-varying parameter identification for load modeling: a deep generative approach," *IEEE Transactions on Industrial Informatics*, vol. 17, no. 3, pp. 1625-1636, Mar. 2021.
[13] P. Dash, S. Mishra, and G. Panda, "Damping multimodal power system oscillation using a hybrid fuzzy controller for series connected facts devices," *IEEE Transactions on Power Systems*, vol. 15, no. 4, pp. 1360-1366, Nov. 2000.
[14] S. Kokoska. (2020, Jan.). Fifty famous curves, lots of calculus questions, and a few answers [Online]. Available: http://citeseerx. ist. psu. edu/viewdoc/download?doi=10.1.1.694.5308&rep=rep1&type=pdf
[15] M. A. Kramer, "Nonlinear principal component analysis using autoassociative neural networks," *AIChE Journal*, vol. 37, no. 2, pp. 233-143, Feb. 1991.
[16] MathWorks. (2020, May). Nonlinear least squares (curve fitting). [Online]. Available: https://www. mathworks. com/help/optim/nonlinear-least-squares-curve-fitting.html
[17] Powertech Labs Inc. (2020, Jan.). TSAT transient security assessment tool. [Online]. Available: https://www.dsatools.com/wp-content/uploads/2020/01/TSAT-Brochure-001.pdf

You Lin received the M.S. degree in electrical engineering from Shandong University, Jinan, China, in 2016. Currently, she is pursuing the Ph.D. degree in electrical engineering at the Department of Electrical and Computer Engineering, Southern Methodist University, Dallas, USA. Her research interests include machine learning and its application in power system load modeling, data analysis, and forecasting.

Jianhui Wang is a Professor with the Department of Electrical and Computer Engineering at Southern Methodist University, Dallas, USA. He has authored and/or co-authored more than 300 journal and conference publications, which have been cited for more than 25000 times by his peers with an H-index of 81. He has been invited to give tutorials and keynote speeches at major conferences including IEEE ISGT, IEEE SmartGridComm, IEEE SEGE, IEEE HPSC and IGEC-XI. He is the past Editor-in-Chief of the IEEE Transactions on Smart Grid and an IEEE PES Distinguished Lecturer. He is also a Guest Editor of a Proceedings of the IEEE special issue on power grid resilience. He is the recipient of the IEEE PES Power System Operation Committee Prize Paper Award in 2015, the 2018 Premium Award for Best Paper in IET Cyber-Physical Systems: Theory & Applications, and the Best Paper Award in IEEE Transactions on Power Systems in 2020. He is a Clarivate Analytics highly cited researcher for the production of multiple highly cited papers that rank in the top 1% by citations for field and year in Web of Science (2018-2020). He is a Fellow of IEEE. His research interests include smart grid, microgrid, cybersecurity, grid resilience, renewable integration, energy economics and policy, electric power systems operations and control, electricity restructuring.